UNCLASSIFIED

AD NUMBER
ADB804797

LIMITATION CHANGES

TO:

Approved for public release; distribution is unlimited.

FROM:

Distribution authorized to DoD only; Administrative/Operational Use; DEC 1940. Other requests shall be referred to National Aeronautics and Space Administration, Washington, DC. Pre-dates formal DoD distribution statements. Treat as DoD only.

AUTHORITY

THIS PAGE IS UNCLASSIFIED

Reproduction Quality Notice

This document is part of the Air Technical Index [ATI] collection. The ATI collection is over 50 years old and was imaged from roll film. The collection has deteriorated over time and is in poor condition. DTIC has reproduced the best available copy utilizing the most current imaging technology. ATI documents that are partially legible have been included in the DTIC collection due to their historical value.

If you are dissatisfied with this document, please feel free to contact our Directorate of User Services at [703] 767-9066/9068 or DSN 427-9066/9068.

Do Not Return This Document To DTIC

REEL - C
358
A.T.I.
9322

UNCLASSIFIED

NATIONAL ADVISORY COMMITTEE FOR AERONAUTICS

WARTIME REPORT

ORIGINALLY ISSUED

DRAG AND PROPULSIVE CHARACTERISTICS OF AIR-COOLED

ENGINE-NACELLE INSTALLATIONS FOR TWO-ENGINE AIRPLANES

By Herbert A. Wilson, Jr., and Robert R. Lehr

Langley Memorial Aeronautical Laboratory
Langley Field, Va.

NACA

WASHINGTON

L — 428

DRAG AND PROPULSIVE CHARACTERISTICS OF AIR-COOLED

ENGINE-NACELLE INSTALLATIONS FOR TWO-ENGINE AIRPLANES

By Herbert A. Wilson, Jr., and Robert R. Lehr

SUMMARY

Research on wing-nacelle propeller arrangements has
been continued in the NACA full-scale wind tunnel with
tests on a model of a two-engine airplane provided with
nacelles varying in diameter from 1.5 to 2.6 times the lo-
cal wing thickness. This model is the same one that was
previously tested with four-engine-nacelle installations,
and the results are directly comparable.

The results show the variation of the nacelle drag
with the ratio of the nacelle diameter to the wing thick-
ness, the effects of the nacelles on the aerodynamic char-
acteristics of the airplane, and the propulsive and the
over-all efficiencies for all the arrangements. The pres-
ent results are combined in some cases with the results of
previous experiments, so that the effect of nacelles is in-
cluded for airplanes ranging from $6\frac{1}{2}$ to 100 tons.

INTRODUCTION

The tendency to increase the power of radial air-
cooled airplane engines without increasing the engine di-
ameter has led to large variations in the size of the
wing nacelles relative to the size of the wing. An in-
vestigation conducted in the NACA full-scale wind tunnel
has dealt with the influence of the ratio of the nacelle
diameter to the wing thickness and of the longitudinal
and vertical propeller location on the drag, the propul-
sive efficiency, and the over-all efficiency of multiengine
airplanes. The effects of the nacelles and the propeller
operation on the lift and the pitching moment of the air-
plane have also been studied. The investigation covered
ratios of the nacelle diameter to the wing thickness vary-
ing from 0.53 to 2.60, representing airplanes of from $6\frac{1}{2}$
to 100 tons gross weight.

By variation of the number and size of the nacelles
installed on the same airplane model, a series of airplanes
has been represented from which directly comparable data
were obtained. The tests of these models were divided into

two groups: The first group, reported in reference 1, con-
sisted of tests of the model with four nacelles of diam-
eters varying from 0.53 to 1.5 times the wing thickness;
the second group, constituting the basis for this report,
covers tests of the model with two nacelles of diameters
varying from 1.5 to 2.6 times the wing thickness.

SYMBOLS

α angle of attack of the fuselage reference axis rela-
tive to the wind axis, degrees

q free-stream dynamic pressure, pounds per square foot

S wing area, square feet

$\bar{c}$ mean chord of wing, area/span, feet

t_w maximum wing thickness (average over nacelle), feet

D_P propeller diameter, feet

D_N maximum nacelle diameter, feet

F maximum cross-sectional area of nacelle, square feet

V air speed, feet per second

L lift, or force normal to the relative wind, pounds

D drag, or force parallel to the relative wind, pounds

D_c power-off drag of model with engine-nacelle installa-
tion, pounds

M pitching moment, pound-feet

$$C_L = \frac{L}{qS}$$

$$C_D = \frac{D}{qS}$$

$\Delta C_D = C_{D_c} - C_{D_w}$ (Subscript w refers to power-off drag of the model with bare wing; subscript c, to power-off drag of model with engine-nacelle installation)

$C_{D_F} = \dfrac{\Delta C_D S}{2F}$

$C_m = \dfrac{M}{q S \bar{c}}$

R   resultant force of a propeller-nacelle-wing combination, pounds

T   thrust of propellers operating in front of a body (tension in propeller shafts), pounds

ΔD increase in drag of the body due to the action of the propellers, pounds

$T-\Delta D$ effective thrust of the propeller-nacelle installation

P   power input to all propellers

$\eta = \dfrac{(T - \Delta D)V}{P}$ propulsive efficiency

$\eta_t = \eta \left(\dfrac{C_{D_w}}{C_{D_c}}\right)$ over-all efficiency

$T'_{c_o} = \dfrac{P\eta_o}{\frac{\rho}{2} V^3 S}$ index thrust coefficient

$\eta_o = \eta$ at $C_L = 0.25$

n   propeller speed, revolutions per second

β propeller-blade angle at 0.75 radius, degrees

δ_f flap deflection from closed position, degrees

MODEL AND TEST EQUIPMENT

The tests were conducted in the NACA full-scale wind tunnel, which is described in reference 2. The model is a metal-covered, midwing monoplane with a span of 37.25 feet. The symmetrical wing sections are tapered in thickness from the NACA 0018 at the root to the NACA 0010 at the tip. The wing plan form tapers 4:1 from a root chord of 7.28 feet, and the wing area is 172 square feet. Split trailing-edge flaps extend over the middle 60 percent of the span with the exception of a short gap at the fuselage. The angle of the wing setting to the fuselage reference line is 4.6°. The principal dimensions of the model and the nacelle for each of the test arrangements are shown in figure 1. Figures 2 to 6 show the model as installed in the full-scale tunnel.

A summary of the nacelle arrangements tested is shown in table I.

TABLE I

Test	Nacelle diameter (in.)	$\frac{D_N}{t_w}$ (1)	Propeller diameter (in.)	$\frac{D_N}{D_P}$	Propeller location (a)	Nacelle position	Details in
1	No cowling - Bare-wing model						fig. 2
2a	20	1.5	48	0.417	0.25c	Center line	fig. 3
2b	20	1.5	48	.417	.25c	Low	fig. 4
3	30.4	2.27	69	.440	.50c	Center line	fig. 5
4	34.7	2.6	84	.413	.50c	Center line	fig. 6

[1] Thickness t_w is the average of wing thickness at the nacelle locations.

[a] Chord c is the local chord at each propeller location.

Power to operate the propellers was furnished for the
20-inch nacelle arrangement by the 25-horsepower alternat-
ing-current motors used in the tests of reference 1, and
for the 30.4-inch and 34.7-inch nacelle arrangements by
15-horsepower motors of lower synchronous speed. For all
three nacelle arrangements, the motors were supported ahead
of the wing and within the nacelles. The propeller speed
was regulated by varying the frequency of the motor-current
supply and was measured with an electric tachometer. Power
output was obtained for the 25-horsepower motors from an
electrical calibration and for the 15-horsepower motors by
measurement of the torque reaction on the motor.

Three sets of propellers, a modified Bureau of Aero-
nautics Drawing No. 4412 two-blade propeller of 48-inch
diameter, a Curtiss 88930 three-blade propeller of 69-inch
diameter, and a Hamilton Standard 1327 two-blade propeller
cut down from an 8- to a 7-foot diameter, were used on the
20-, the 30.4-, and 34.7-inch nacelles, respectively.

The contour of the cowlings and their relative dimen-
sions are given in figure 7 as fractions of the cowling
diameter. These cowlings were geometrically similar to
those used in the previous series of tests (reference 1)
and to the one designated cowling C in reference 3. The
shapes of the nacelles were designed in each case to avoid
flow separation on the afterbody. At the intersection of
the nacelle and the wing plasticine fillets of small radi-
us were used to provide a smooth fairing.

Perforated metal plates, the resistance of which was
changed to a value of conductance K (reference 4)
of approximately 0.10, simulated the engine. The
exit slot of the cowling was proportioned to give a
pressure drop of $0.030q$ across the engine; it was
assumed that a means of exit-slot adjustment such as
flaps would be provided for other flight conditions.
For the tests with no cooling air, the exit slot was
sealed to prevent any air flow through the cowling.
This method was found to give more consistent results
than sealing the perforation in the metal plates of
the engine, as was done for the tests of reference 1;
the improvement can be attributed to a better flow
condition at the exit slot.

6

TESTS

With propellers removed from the model, measurements
of aerodynamic characteristics were made at an air speed
of about 60 miles per hour for each of the nacelle instal-
lations over an angle-of-attack range from zero lift
through the stall. Scale effect on the drag at low lift
coefficients was also measured over a range of air speeds
from 30 to 100 miles per hour.

With the propellers operating, propulsive character-
istics of the nacelle-propeller installations were deter-
mined for the attitude in which the thrust axes were par-
allel to the relative wind and for lift coefficients ap-
proximating those for the high-speed and the climbing con-
ditions. The power-on measurements included the power in-
put to the propellers and the propeller speed as well as
the usual aerodynamic forces and moments. For the propul-
sive efficiency tests, the V/nD was varied by increasing
the air speed from 30 to 100 miles per hour and then by
decreasing the propeller speed at the maximum air speed
until zero torque was obtained. The effect of propeller
operation on the lift and on the pitching moment was de-
termined at a test air speed of approximately 60 miles per
hour for the maximum thrust permitted by the set-up and
for an intermediate thrust condition.

POWER-OFF CHARACTERISTICS

The aerodynamic characteristics of the two-engine
model with the propellers removed are shown in figures 8
to 12 for the various arrangements tested. These data
were obtained at a tunnel air speed of about 60 miles per
hour, which corresponds to a Reynolds number of about
2,500,000 based on the average wing chord of 4.62 feet.
The coefficients are based on a wing area of 172 square
feet and are corrected for wind-tunnel effects. Pitching-
moment coefficients are computed about a center of gravity
located as shown in figure 1.

Drag.- Scale effects on the airplane drag coefficients
for the nacelle arrangements and for the model without na-
celles, tested at an assumed high-speed lift coefficient of
0.25 are given in figure 13. A comparison of the curves
for the various nacelle installations with those for the

bare wing shows that the drag increment due to the nacelles is more or less independent of the test air speed within the range covered.

The variation of the nacelle drag increment per nacelle $\Delta C_D/2$ with the ratio of the nacelle-diameter to the wing thickness D_N/t_w is shown in figures 14(a), (b), (c), and (d) for the present tests at lift coefficients of -0.04, 0.25, 0.5, and 0.7, together with similar data from the earlier tests of reference 1. The propeller location for nacelle arrangements with values of D_N/t_w of 2.27 and 2.80 was 0.50c ahead of the leading edge of the wing as compared with a position of 0.40c for the other nacelles of figures 14(c) and (d). The difference in drag between the nacelles with the propeller positions of 0.40c and of 0.50c has been disregarded in the discussion of the variation of the nacelle drag coefficient and will be examined later. The increase in the total drag due to nacelles of large relative diameter as well as the importance of the drag due to the flow of the cowling air for large values of D_N/t_w is clearly shown in figure 14.

The nacelle drags are also shown in terms of the nacelle drag coefficient C_{D_N} in figure 15, from which figure the drag of conventional nacelle and cowling installations can be predicted. There is a large increase in nacelle drag coefficient with lift coefficient for small values of D_N/t_w. As the value of D_N/t_w increases, the nacelle drag coefficient tends to approach a constant value and to become considerably less dependent on the lift coefficient and the propeller position.

The nacelle drags without cooling air flowing were considerably smaller for the two-nacelle tests than for the four-nacelle tests of reference 1. This difference is particularly noticeable for the 20-inch nacelles with the 0.25c propeller position because a direct comparison is shown. The decrease in nacelle drags is attributed to sealing the cowling exit for the present tests rather than sealing the perforated metal plates, thus eliminating secondary flows due to pressure differences around the periphery of the cowling exit.

Calculations of the drag due to forcing air through the cowling and the perforated plate simulating the engine, as outlined in reference 4, give increases in the

nacelle drag coefficient of 0.020 and 0.014 for the 34.7-
and the 30.4-inch nacelles, respectively, that check re-
markably well with the values of 0.019 and 0.014 from the
data of figure 15.

An unexpected decrease in drag was shown by the 20-
inch nacelles in the low position (fig. 13). This de-
crease is inconsistent with the results of recent tests
made in the NACA 8-foot high-speed tunnel (reference 5)
that show a 2-percent increase in the airplane drag for
lowering the nacelle. For the tests of reference 5, the
lowered nacelle was geometrically similar to the center-
line nacelle; whereas, in the present tests the nacelle
afterbody was faired to provide additional space in the
nacelle for housing the landing gear. This requirement of
space made it necessary to elongate the nacelle and to
fair from the circular engine section to a vertical line
at the tail. It is believed that the more gradual fairing
of the low nacelle caused less interference between the
wing and the nacelle on the lower surface and that lower-
ing the nacelle decreased the interference on the upper
surface of the wing to a low value. This conclusion is
partially verified by the fact that the drag for the low-
ered nacelle approaches more nearly the skin-friction drag
for a corresponding amount of surface in turbulent flow.

Maximum lift.- The maximum lift coefficient was
slightly decreased (about 1 percent) by the addition of the
nacelles to the airplane. Table II summarizes the maximum
lifts for all the test arrangements.

TABLE II

Values of Maximum Lift Coefficient

| D_N/t_w | Propeller location | Flap deflection, δ_f | | |
		0°	60°	Vertical position
Bare wing		1.29	1.82	
1.50	0.25c	1.28	1.77	Center line
1.50	.25c	1.28	1.76	Low
2.27	.50c	1.27	--	Center line
2.60	.50c	1.26	--	Center line

L-428

A comparison of the values for the current tests with those for the tests of reference 1 shows a considerable difference in the effect of the nacelles on maximum lift. Adding four 20-inch nacelles to the model gave a decrease in maximum lift of 9 percent; this decrease is inconsistent with the results of the two-nacelle tests. Tuft surveys (fig. 16) show that the nacelle has a marked effect on the direction of flow over the top of the wing, and it is reasonable to conclude that two nacelles only a short distance apart have a mutual interference flow that, at high angles of attack, causes an early separation on the upper surface of the wing. It is also evident from the two-engine tests that the interference is not serious for an isolated wing nacelle.

Lift-drag ratio.- The range of an airplane is about proportional to the value of the maximum lift-drag ratio, which decreases rapidly with increasing D_N/t_w, as shown in figure 17. The maximum L/D for the 20-inch nacelle $(D_N/t_w = 1.5)$ is 15 percent lower than that for the bare wing while the L/D 34.7-inch nacelle $(D_N/t_w = 2.6)$ is 20 percent lower. The four-engine data of reference 1, also included in figure 17, show the lift-drag ratio for the four 20-inch-nacelle installations to be approximately 25 percent less than for the bare wing.

Pitching moment.- The destabilizing effect of large nacelles is apparent in figure 18, in which the slopes of the pitching-moment coefficient curves are plotted against D_N/t_w. The slopes were read over the straight portions of the pitching-moment curves at values of α between -5° and 5°, the decreased stability being indicated by lower values of negative slope. The curves include, in addition to the results of the present nacelle and bare-wing tests, similar data obtained with four nacelles in reference 1. The results were found to be much more critical for the four-nacelle conditions.

The decrease noted in the slope of the pitching-moment curve is attributed to the forward movement of the aerodynamic center of the wing due to the addition of the nacelles ahead of the leading edge. Consequently, moving the nacelles ahead from a propeller position of 0.25c to one of 0.40c or 0.50c further accentuates the destabilizing effect of the nacelles.

PROPULSIVE AND OVER-ALL EFFICIENCIES

The nacelle drag coefficients alone are an insufficient basis for comparison of the various nacelle-propeller installations. The installations are more properly compared by means of an over-all efficiency that includes the nacelle drag increment measured with the propeller removed as well as the propulsive efficiency. This over-all efficiency η_t is defined as the ratio of the towline power required for the model without nacelles at a given level-flight speed to the actual power input required at this speed by the model with the nacelle-propeller installation. The over-all efficiency is therefore written

$$\eta_t = \eta \left(\frac{C_{D_W}}{C_{D_C}} \right)$$

The propulsive efficiency η is the ratio of the effective thrust power to the power input and may be calculated from the relation

$$\eta = \frac{(T - \Delta D)\,V}{P}$$

The value of the effective thrust, $(T - \Delta D)$, can be computed from the wind-tunnel data by the relationship

$$T - \Delta D = D_C + R$$

in which D_C and R are, respectively, the values of the drag for propeller-removed and propeller-operating conditions.

The drag increment included in the effective thrust is caused by the slipstream over the wing; in like manner a lift increment is attributed to the propeller operation. In order to correct for this lift change, D_C and R were both measured at the same lift coefficient rather than at the same angle of attack.

Propulsive Efficiencies

Data have been obtained from the tests to show the effect on the propulsive efficiency of variations in the pro-

peller blade angle, the nacelle diameter, and the lift coefficient.

Propeller blade angle.- The values of the propulsive efficiencies measured for the various nacelle-propeller combinations are shown in figures 19 to 22. The maximum propulsive efficiencies occur at a blade angle β of about 30°; the envelopes of the propulsive-efficiency curves are reasonably flat, however, showing only slight variations in efficiencies with a variation in β of ±10° from the optimum.

The results show that neither the blade angle for maximum efficiency nor the quantitative value of maximum efficiency varies appreciably from that of the previous study of the four nacelle propeller installations.

Nacelle diameter.- A variation in the ratio of the nacelle diameter to the wing thickness has little effect on the maximum propulsive efficiency. Changing the vertical position also has a negligible effect on the maximum efficiency except to change slightly the V/nD at which maximum efficiency occurs. The efficiency at a lift coefficient of -0.04 for the 34.7-inch nacelles is approximately 2 percent lower than that for the 20-inch nacelles and about 1 percent lower than that for the 30.4-inch nacelles.

Lift coefficients.- The variations in the propulsive efficiencies with airplane lift coefficient are also included in figures 19 to 22 for blade angles of 20°, 30°, and 40°. The maximum propulsive efficiency occurs at a lift coefficient of -0.04, in which case the nacelle axis was approximately parallel to the air stream. The propulsive efficiency in all cases except for the 20-inch nacelle with the blade angle set at 30° is 2 percent greater at the lift coefficient -0.04 than at 0.25. For the 20-inch nacelle with a blade angle of 30° the propulsive efficiency is the same for the two lift coefficients in either the center line or the lowered nacelle position.

Over-All Efficiencies

The over-all efficiencies for the conditions investigated during the present series of tests together with those of the previous series (reference 1) are presented in figure 23.

It will be noted that there is a 1- to 2-percent decrease in the over-all efficiency for the 0.40c propeller position. The decrease is probably due to the increased skin friction of the longer nacelle. It will also be observed that the over-all efficiency for the two-engine installation is considerably higher than that for the four-engine installation, especially at larger values of D_N/t_w. This difference in over-all efficiency is the result of the lower drag obtained with two nacelles and indicates the desirability of using the smallest possible number of power units for a given total power output.

Variations of the maximum over-all efficiency with lift coefficient for the two-engine data of the present tests and for the four-engine data of the previous series (reference 1) are plotted in figure 24. In all cases shown, the lowest efficiencies exist at the high-speed condition; the efficiencies increase as the lift coefficient either increases or decreases from the high-speed condition. This increase in efficiency is more rapid with the 30.4- and the 34.7-inch nacelles, because of a smaller variation in drag with angle of attack for the larger nacelles.

POWER-ON CHARACTERISTICS

The effect of propeller operation on the aerodynamic characteristics of an airplane is primarily dependent on the amount of thrust delivered by the propellers and, for a given thrust, is relatively independent of moderate changes in blade angle, V/nD, propulsive efficiency, and propeller diameter. In order to describe the conditions of propeller operation, use is made of an index thrust coefficient that takes the form

$$T'_{c_0} = \frac{P\eta_0}{qSV}$$

in which η_0 is the propulsive efficiency at $C_L = 0.25$ for the conditions of V/nD and blade angle at which the tests were made. The index thrust coefficient has the characteristics and the form of a drag coefficient and is essentially independent of the combination of V/nD and blade angle that produces the thrust; it is equal to the amount of drag that the thrust would counterbalance at the

standard or index condition and, at any other value of
lift coefficient, differs from the true thrust coefficient
only by the variation in propulsive efficiency between the
two conditions.

The effect of propeller operation on the maximum lift
is given in figures 25 and 26 for the 20-inch and the 30.4-
inch nacelle installations. As the index thrust coeffi-
cient increases, the slope of the lift curve increases
slightly and the maximum lift increases rapidly. The rate
of increase in maximum lift coefficient is largest for
values of T'_{c_0} between 0 and 0.05, owing to the effect of
the slipstream in decreasing the wing-nacelle interference.

The effects of the propeller operation on the pitching-
moment coefficient, for the various thrust coefficients
and two nacelle installations, are shown in figures 27 and
28. The principal effect of propeller operation is to
change the elevator angle required for balance. The curves
are similar throughout the normal range of angles of attack
and are very much like those that would be obtained by var-
ying the tail setting. Increasing the nacelle size from
20 inches to 30.4 inches decreases the slope of all of the
power-on pitching-moment curves. With the largest value of
T'_{c_0} for each case, and especially with the larger nacelle,
the stability becomes critical at the higher angles of at-
tack.

PRESSURE DISTRIBUTION

The pressure distribution on the under side of the
20-inch and the 34.7-inch nacelles is given in figures 29
and 30, respectively. These data may be used as a guide
in designing trapdoors on the bottom of conventional na-
celles. Similar data for fuselages are given for a large
range of Mach numbers in reference 6.

Pressures are given in terms of the pressure coeffi-
cient, $P = \dfrac{p - p_0}{q}$ (in which p is the local pressure
and p_0 is the free-stream static pressure), plotted nor-
mal to the surface of the nacelle. The results are plot-
ted to give the distribution over four cross-sectional
planes of the nacelles, located as shown in figures 29(b)
and 30(b), between the leading edge of the wing and the

14

trailing edge of the nacelles. The pressure distribution
over the longitudinal sections is also shown in figures
29(a) and 30(a) for the center-line sections to give an
indication of the fore-and-aft pressure variations.

CONCLUSIONS

1. The over-all efficiency of the two-engine model
decreased linearly with an increase in the ratio of the
nacelle diameter to the wing thickness.

2. The propulsive efficiencies were substantially
the same for all nacelle arrangements.

3. The static longitudinal stability was adversely
affected by the addition of the nacelles to the wing and
the operation of the propellers.

4. The addition of the two nacelles to the wing de-
creased the maximum lift by only about 1 percent.

Langley Memorial Aeronautical Laboratory,
    National Advisory Committee for Aeronautics,
        Langley Field, Va.

REFERENCES

1. Silverstein, Abe, and Wilson, Herbert A., Jr.: Drag
   and Propulsive Characteristics of Air-Cooled Engine-
   Nacelle Installations for Large Airplanes. NACA
   Rep. No. 746, 1942.

2. DeFrance, Smith J.: The N.A.C.A. Full-Scale Wind Tun-
   nel. Rep. No. 459, NACA, 1933.

3. Robinson, Russell G., and Becker, John V.: High-
   Speed Tests of Radial-Engine Cowlings. NACA
   Rep. No. 745, 1942.

4. Theodorsen, Theodore, Brevoort, M. J., and Stickle,
   George W.: Full-Scale Tests of N.A.C.A. Cowlings.
   NACA Rep. No. 592, 1937.

5. Becker, John V., and Leonard, Lloyd H.: High-Speed
   Tests of a Model Twin-Engine Low-Wing Transport
   Airplane. NACA Rep. No. 750, 1942.

6. Delano, James B.: Pressure Distribution on the Fuse-
   lage of a Midwing Airplane Model at High Speeds.
   NACA TN No. 890, 1943.

Horizontal
tail area,
28 sq ft

(a)
The
28-inch
nacelle;
$D_N/t_w = 1.50$

58⅛"

73¾"

29"

20"

.25c

.25c

6.9"

4½"

8.45"
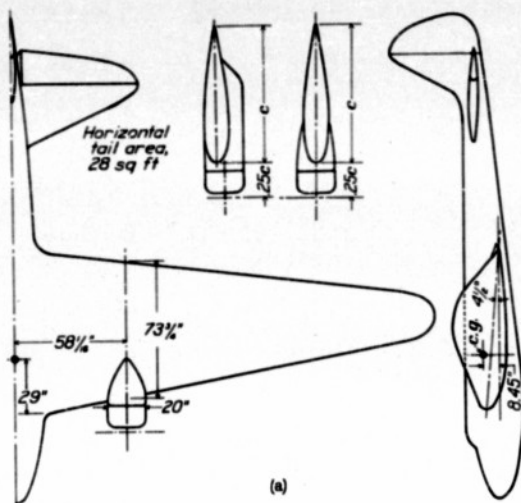
(a)

(b)
The
30.4-inch
nacelle;
$D_N/t_w = 2.27$

58⅛"

73¾"

29"

30.4"

c

.50c

(b)
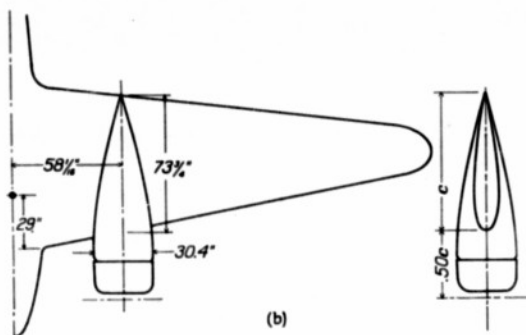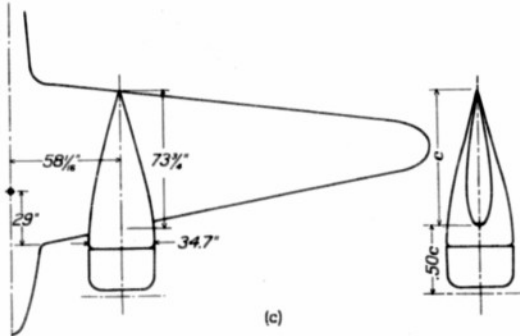
Figure 1.-

Diagram
of model
showing
arrangements
of the
nacelles.

(c)
The
34.7-inch
nacelle;
$D_N/t_w = 2.60$

58⅛"

73¾"

29"

34.7"

c

.50c

(c)

17

L-478
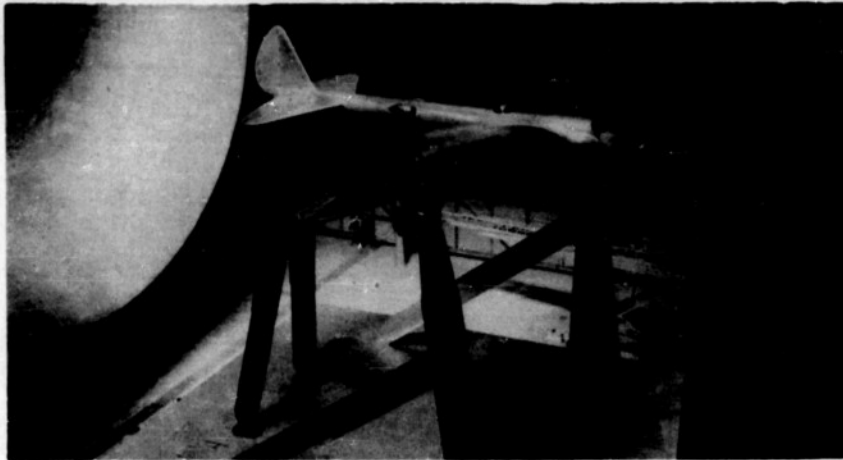
Figure 2.- Installation of model without nacelles in the NACA full-scale tunnel.
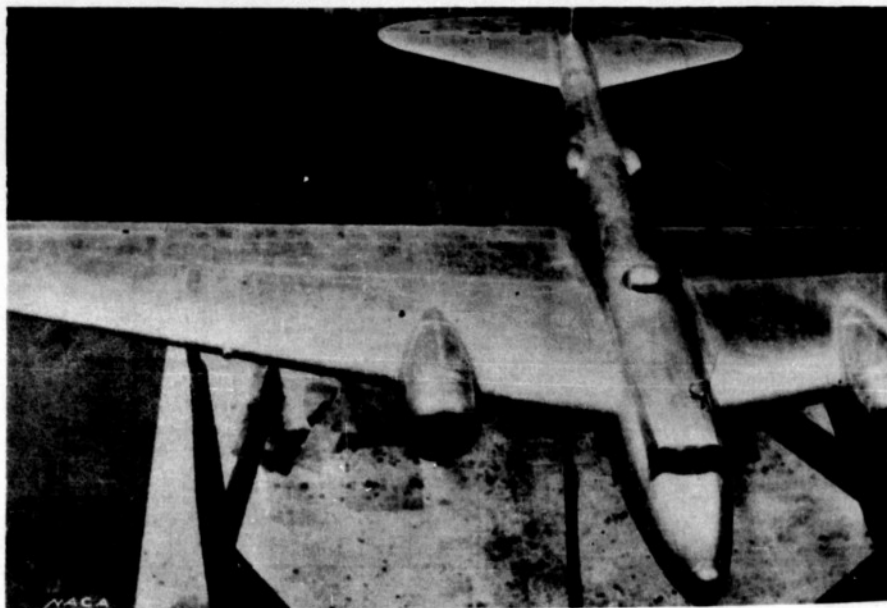
Figure 3.- Installation of model with 20-inch nacelles (center-line position) in the NACA full-scale wind tunnel.

NACA

Figure 4.- Installation of model with 20-inch nacelles (low position) in the
NACA full-scale wind tunnel.

Figure 5. - Installation of model with 30.4-inch nacelles (center-line position)
in the NACA full-scale wind tunnel.

Figure 6.- Installation of model with 34.7-inch nacelles (center-line position) in the NACA full-scale wind tunnel.
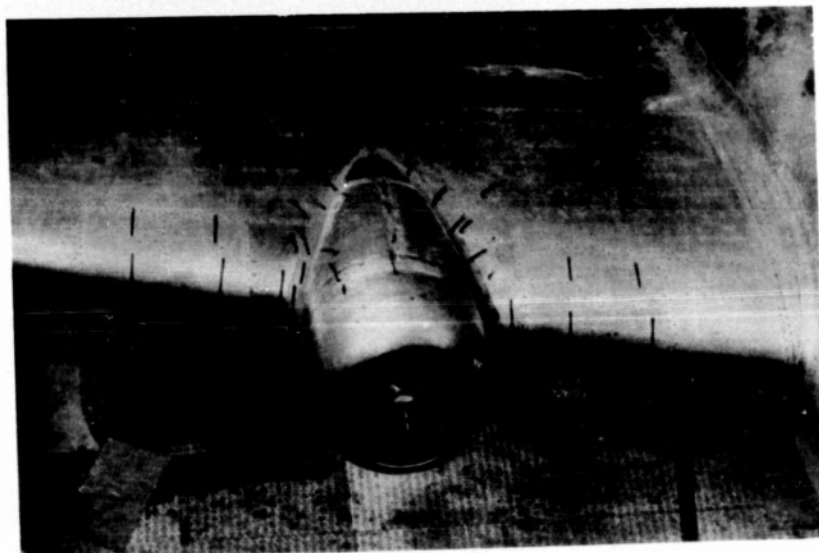
Figure 16.- Air flow over upper surface of wing and nacelle. The 20-inch nacelle: 0.25c propeller location: a = 12°

L-428

Cowling profile			
x/D_N	y/D_N	x/D_N	y/D_N
0.000	0.350	0.115	0.460
.005	.378	.135	.467
.010	.387	.154	.474
.019	.399	.192	.485
.038	.416	.231	.493
.058	.431	.269	.496
.077	.441	.308	.500
.096	.452	.335	.500
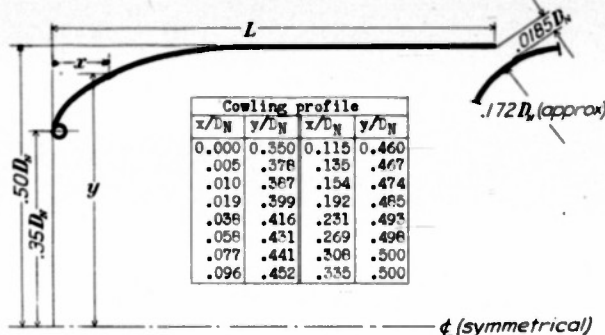
Figure 7.- Dimensions of cowling and cooling arrangement.

L = 11.06 in. for 20.0 in. nacelle
" 16.69 " " 30.4- " "
" 22.00 " " 34.7- " "
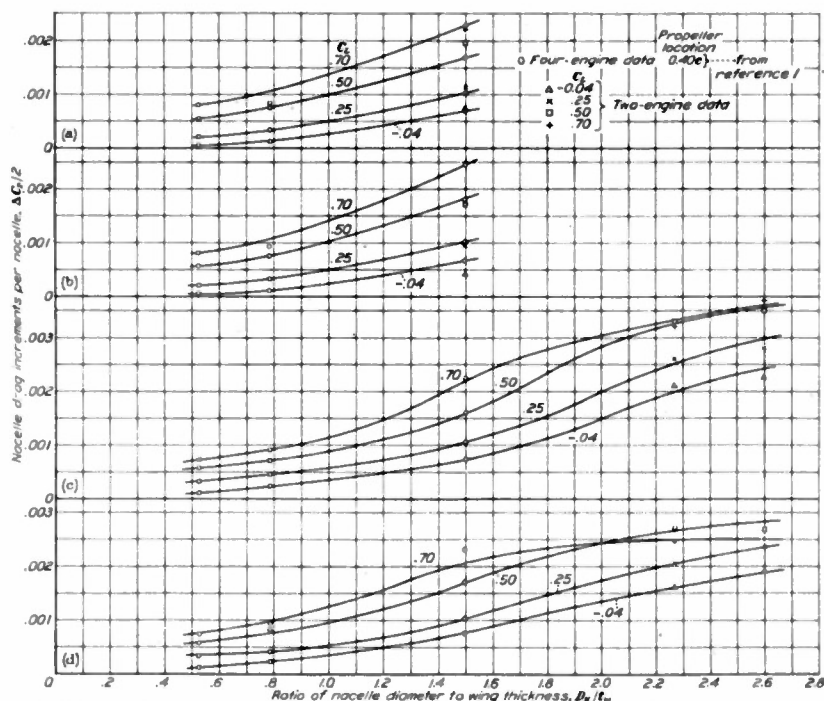
(a) Air flowing through cowling; propeller location, 0.25c. (b) Cowling closed; pro-
peller location, 0.25c. (c) Air flowing through cowling; propeller location, 0.50c.
(d) Cowling closed; propeller location, 0.50c.

Figure 14.- Drag increment due to each nacelle, $\Delta C_D/2$, for nacelles of various size and
various lift coefficients. Test air speed, 100 mph.
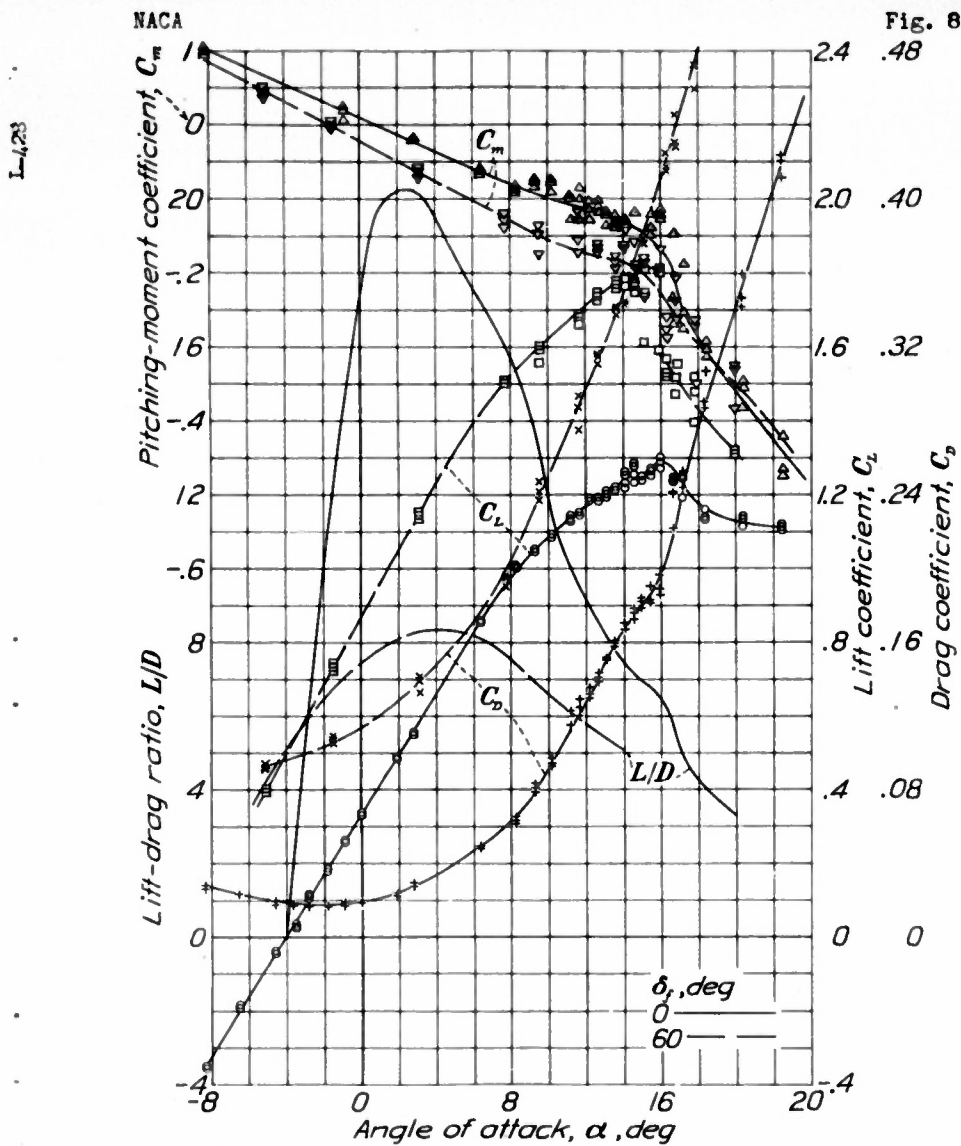
Figure 8.- Aerodynamic characteristics of model without nacelles.
Approximate test air speed, 58 mph.
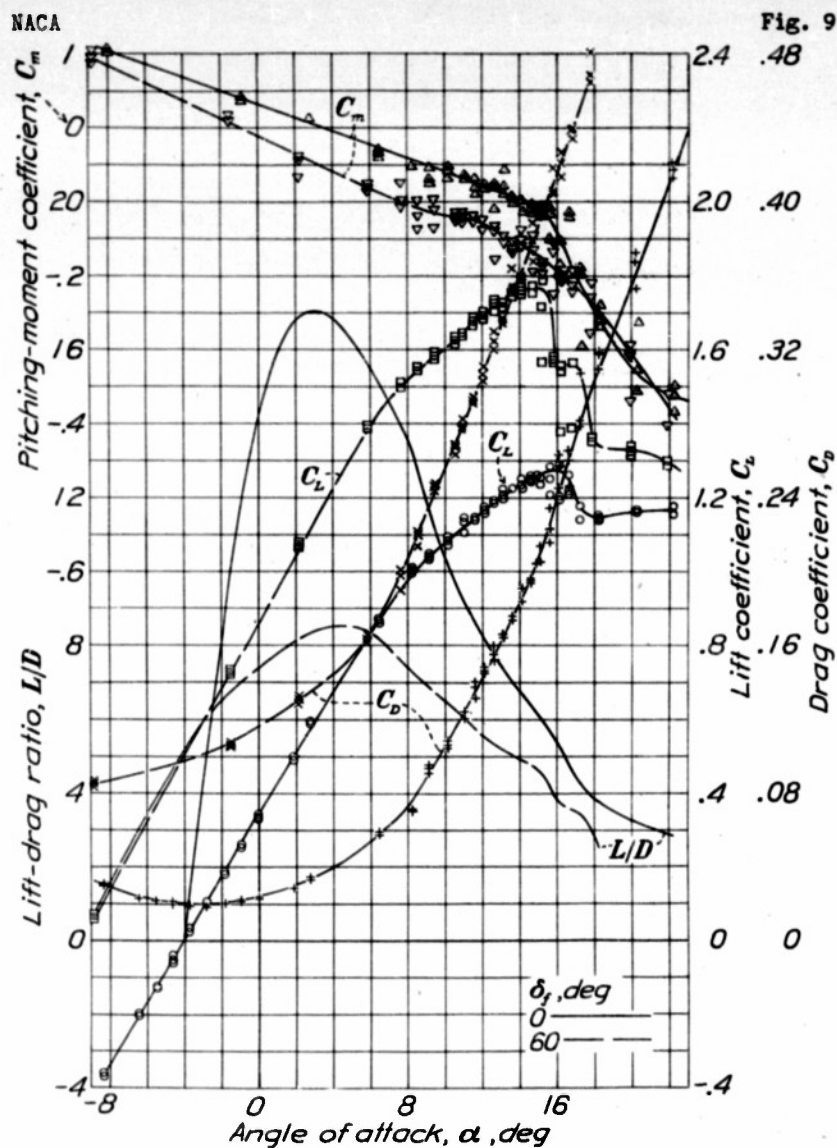
Figure 9.- Aerodynamic characteristics of model with 20-inch nacelles in center-line position. Approximate test air speed, 58 mph.
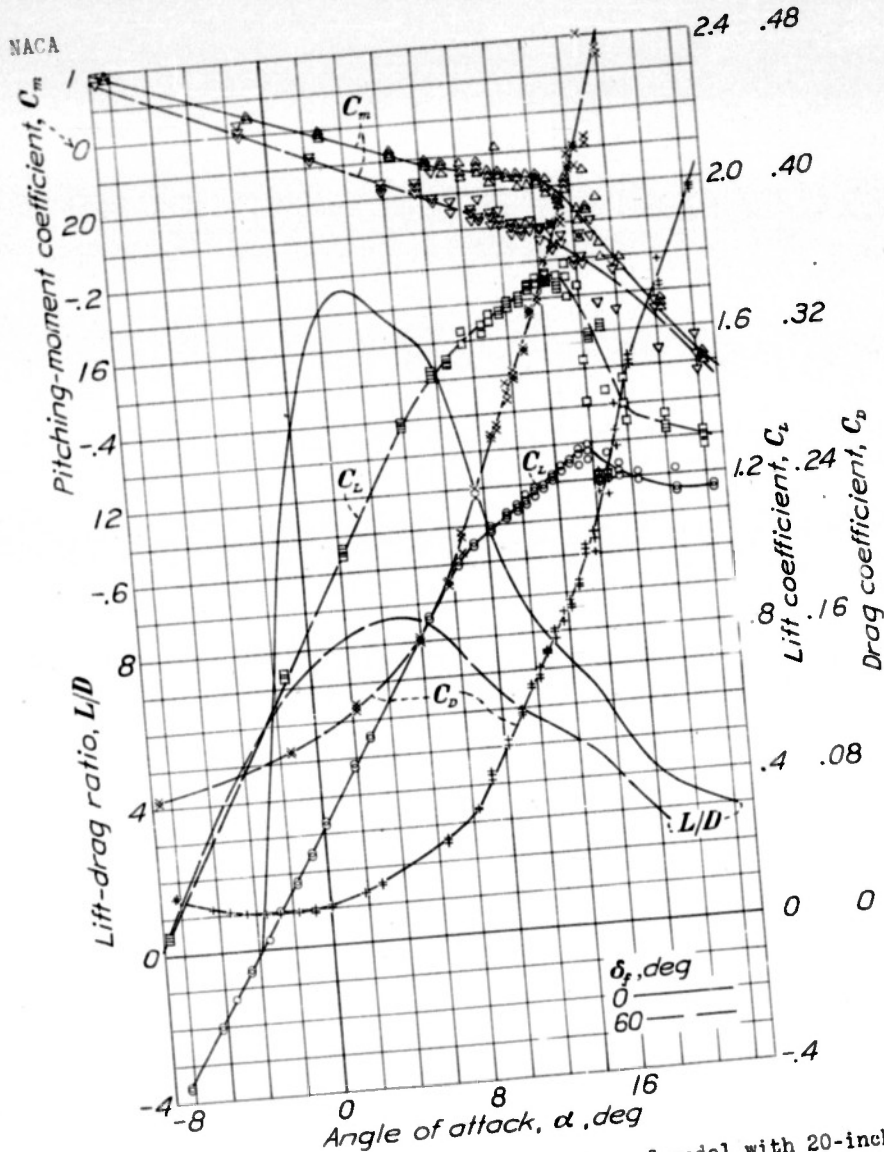
Figure 10.- Aerodynamic characteristics of model with 20-inch
nacelles in low position. Approximate test
air speed, 58 mph.

Fig. 11
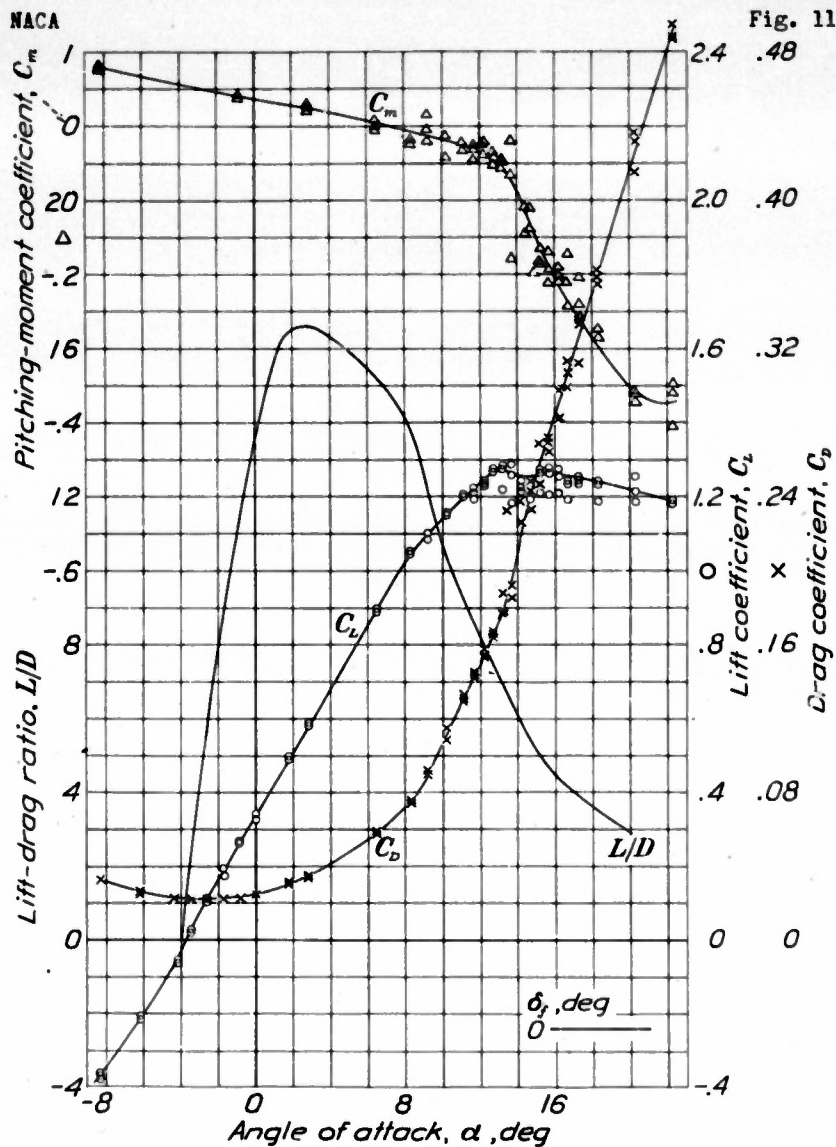
Figure 11.- Aerodynamic characteristics of model with 30.4 inch
nacelles. Approximate test air speed, 58 mph.

Fig. 12
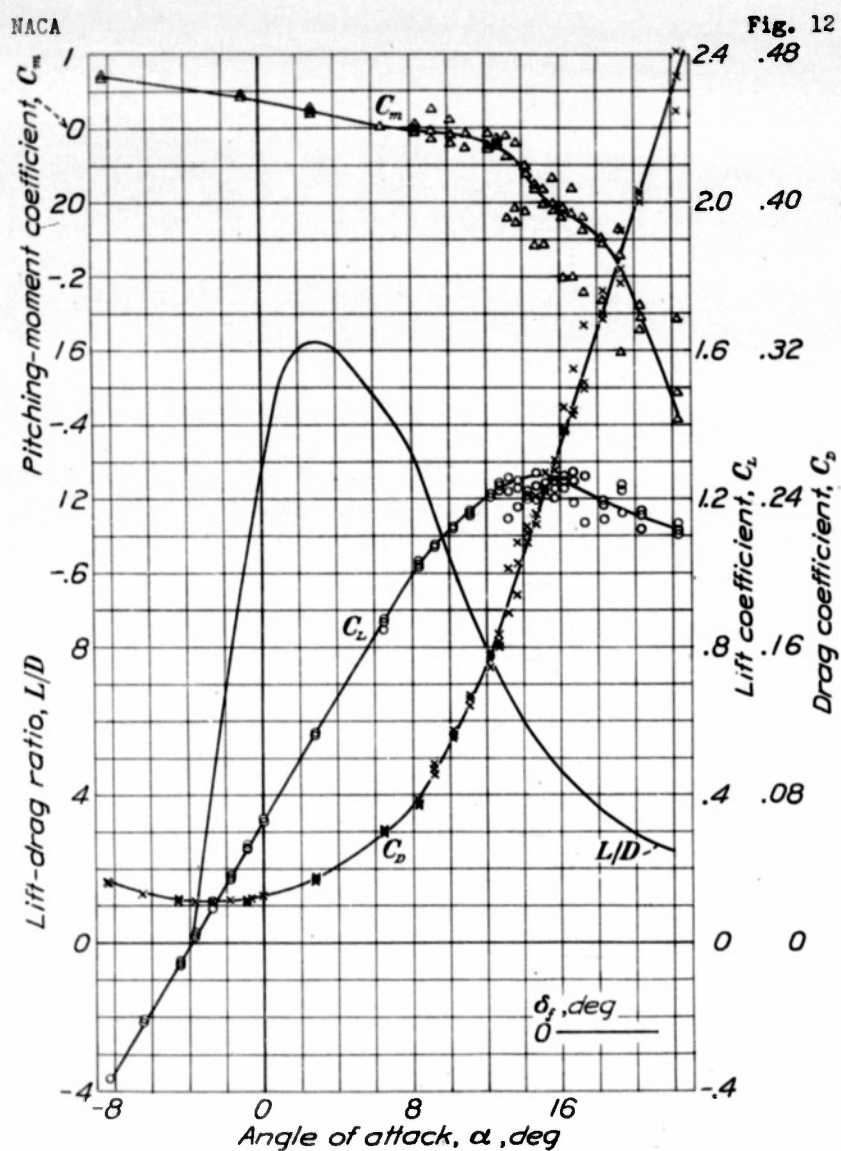
Figure 12.- Aerodynamic characteristics of model with 34.7 inch nacelles. Approximate test air speed, 58 mph.

Fig. 13

L-428
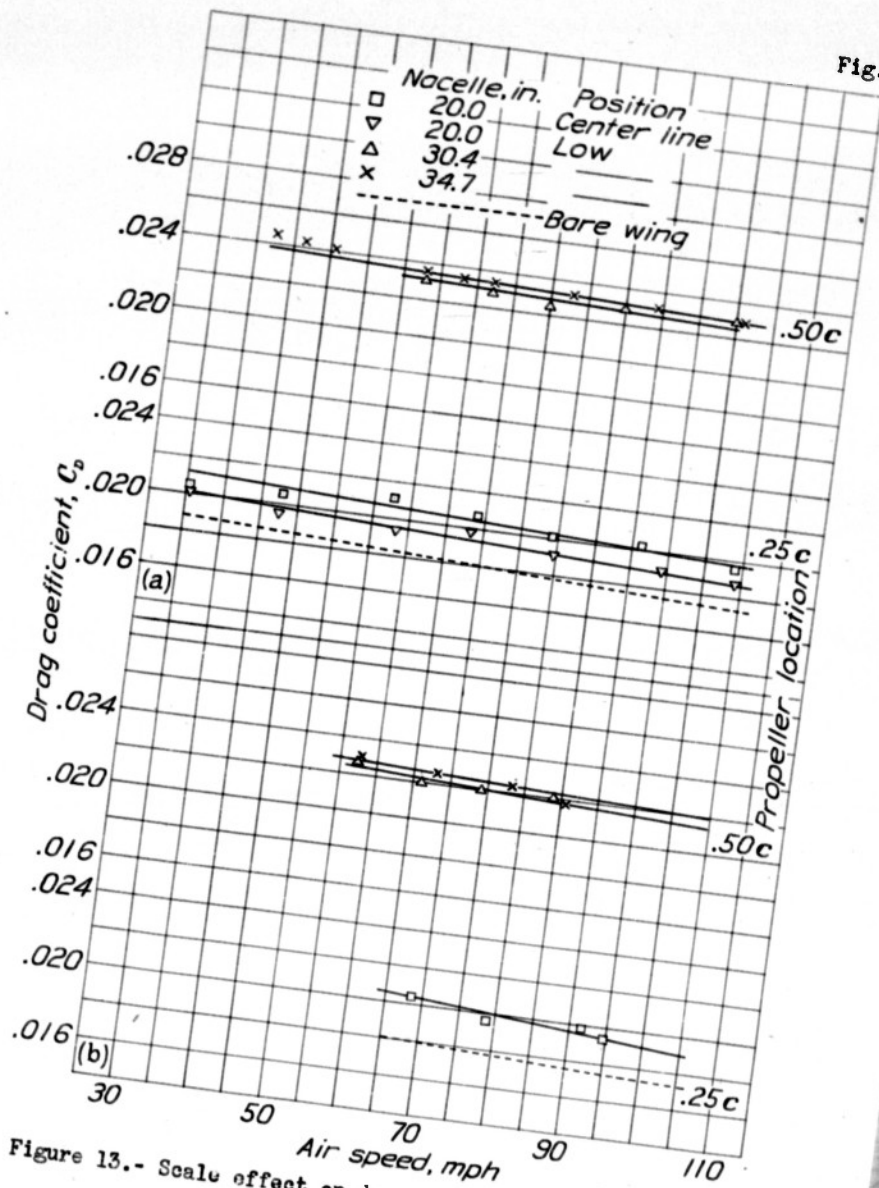
Figure 13.- Scale effect on drag coefficient at $C_L = 0.25$.

(a) Air flowing through cowling   (b) Cowling closed
Figure 15.- Nacelle drag coefficient for various size nacelles and lift coefficients.
            Center-line nacelles.

Figure 17.- Variation of the maximum lift-
            drag ratio of the model for
            various nacelle sizes.

Figure 18.- Variation of the slope of the
            pitching-moment curve of the
            model for various nacelle sizes.
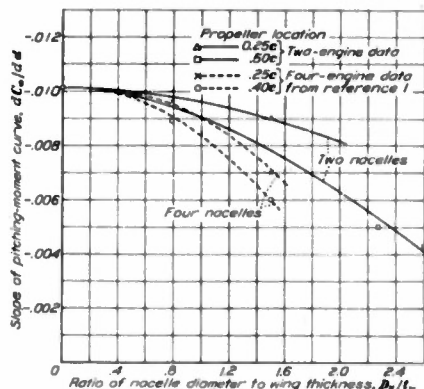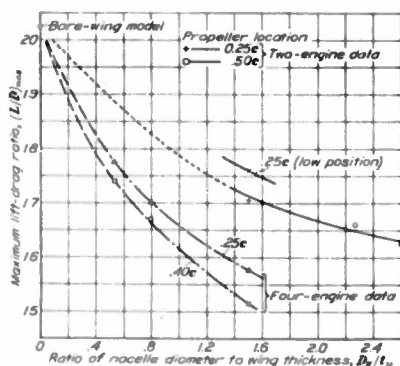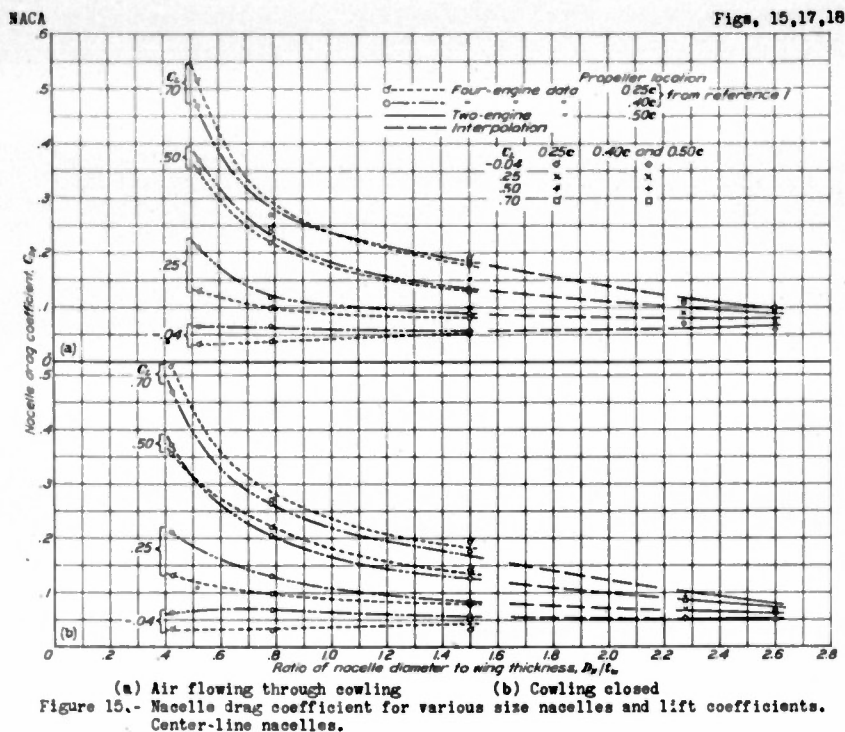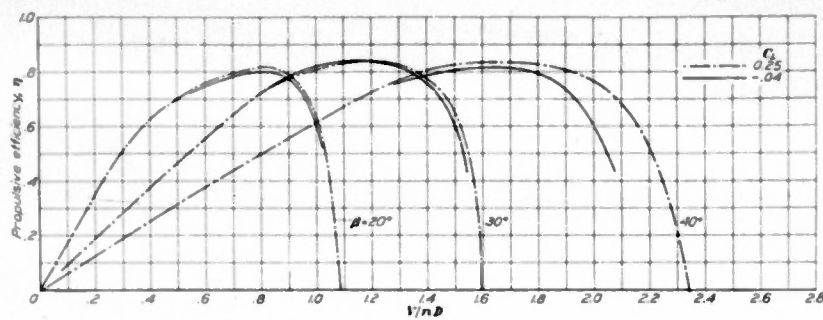
Figure 19.- Variation of propulsive efficiency with blade angle for the 20-inch nacelles in center-line position. 0.25c propeller location; air flowing through cowling.
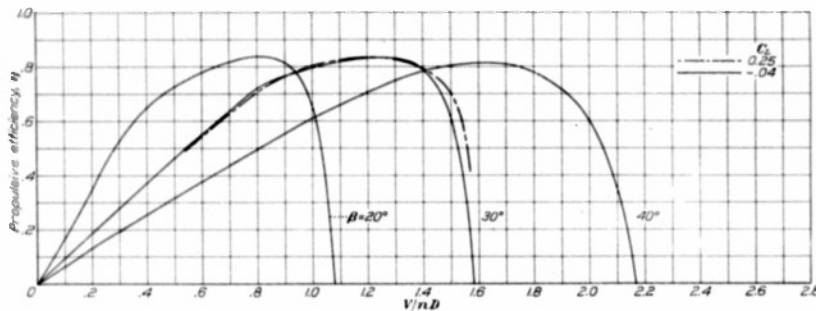
Figure 20.- Variation of propulsive efficiency with blade angle for the 20-inch nacelles in low position. 0.25c propeller location; air flowing through cowling.
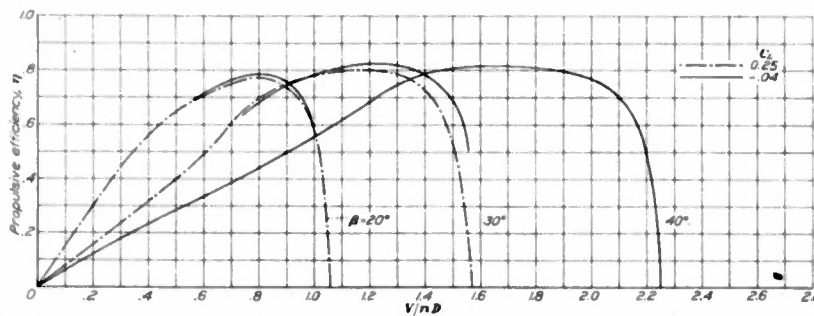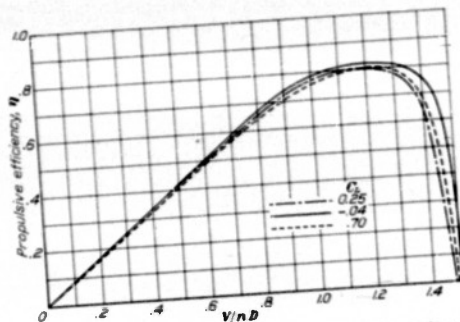

Figure 21.- Variation of propulsive efficiency with blade angle for the 30.4-inch nacelles 0.50c propeller location; air flowing through cowling.

84

Figure 22.- Variation of propulsive efficiency with lift coefficient
for the 34.7-inch nacelles. 0.50c propeller location;
β, 30°; air flowing through cowling.
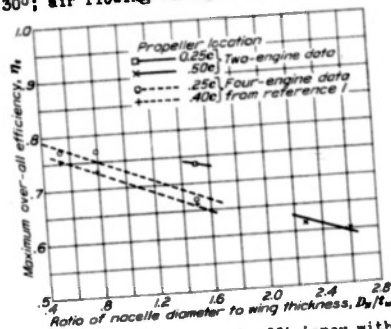
Figure 23.- Variation of maximum over-all efficiency with nacelle size.
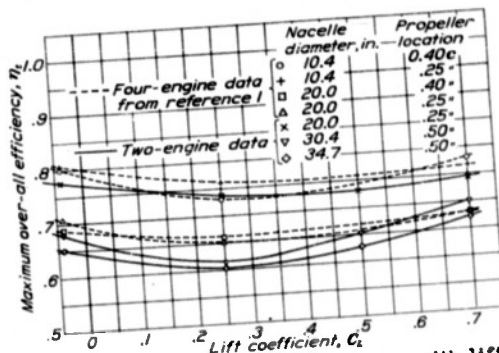C_L, 0.25; β, approximately 30°; air flowing through cowling.

Figure 24.- Variation of maximum over-all efficiency with lift coefficient.
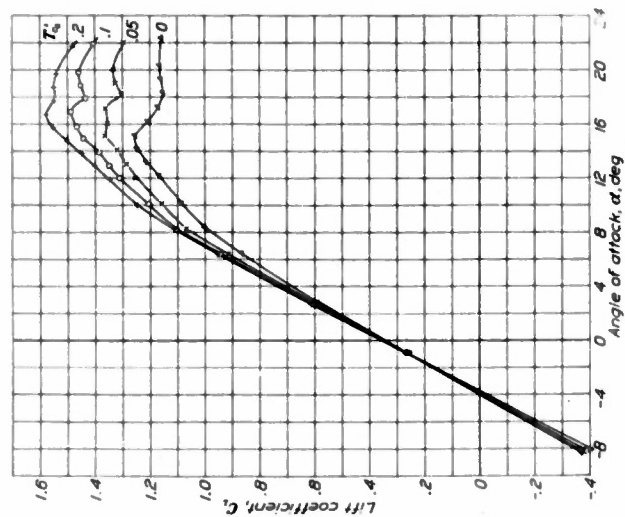Various nacelle arrangements; β, approximately 30°.
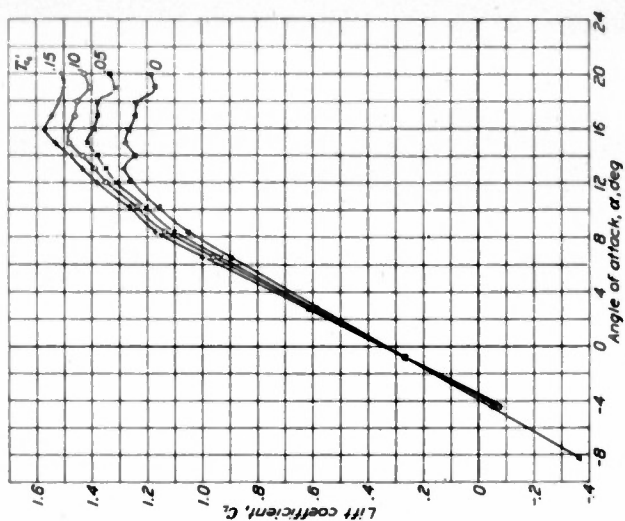
L-428

Figure 26.- Effect of propeller operation on lift coefficient of the model for various index thrust coefficients. The 34.7-inch nacelles; 0.50c propeller location; $\delta_f = 0^\circ$.

Figure 25.- Effect of propeller operation on lift coefficient of the model for various index thrust coefficients. The 20-inch nacelles in low position; 0.25c propeller location; $\delta_f = 0^\circ$.
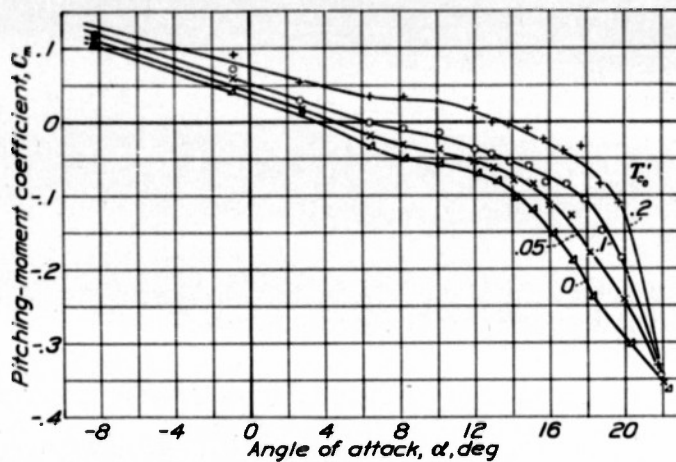
Figure 27.- Variation of pitching-moment coefficient of the
            model with index thrust coefficient. The 20-inch
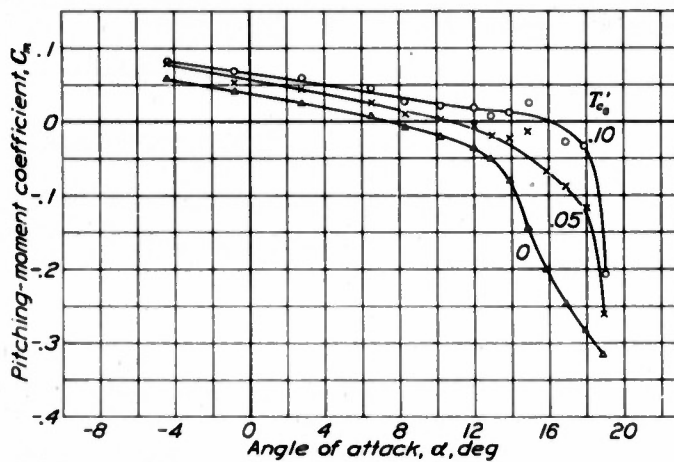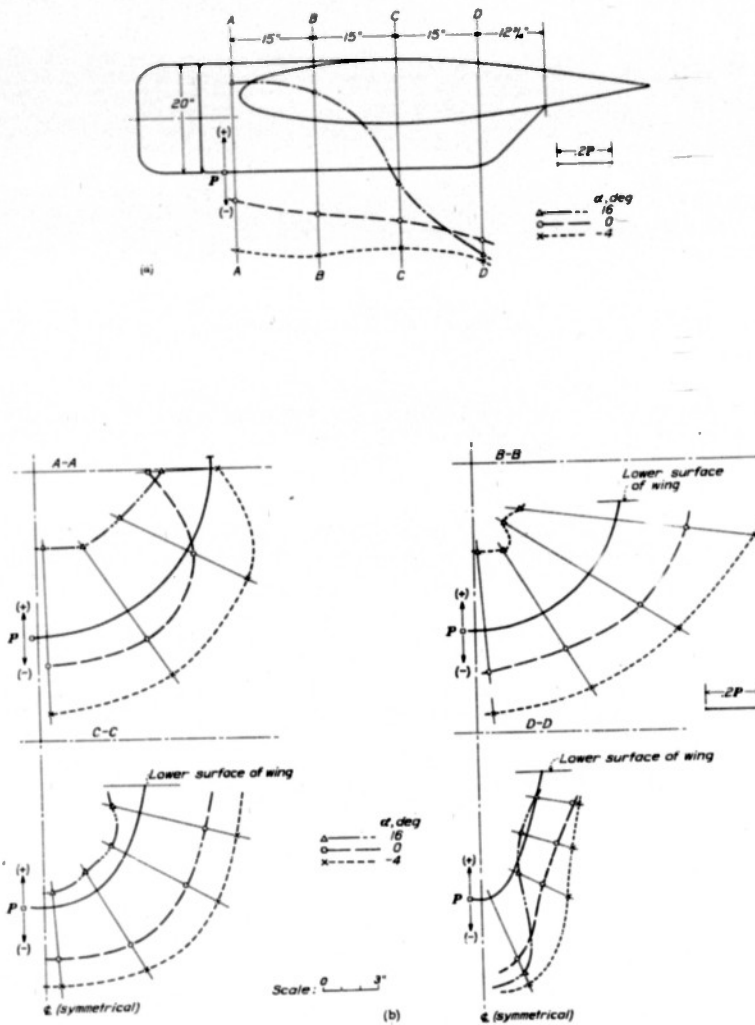nacelles in center-line position. 0.25c propeller location.

Figure 28.- Variation of pitching-moment coefficient of the
            model with index thrust coefficient. The 34.7-inch
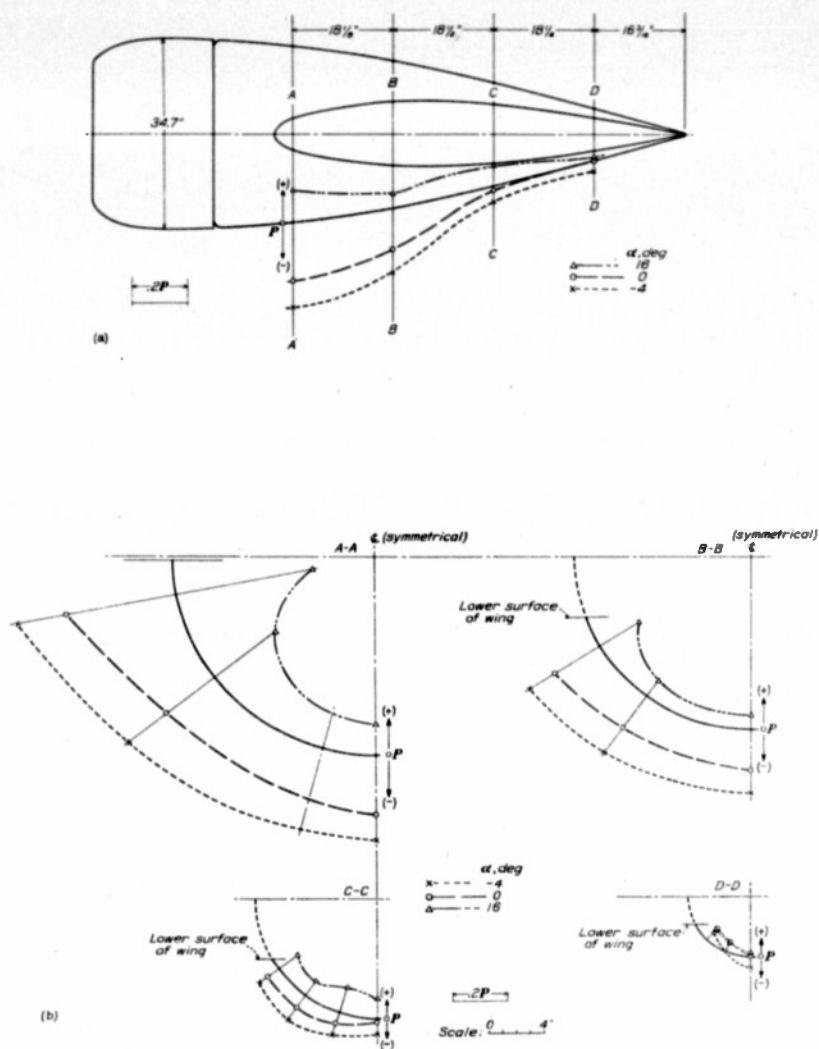nacelles; 0.50c propeller location.

Fig. 29

L-428

(a) Longitudinal sections.

(b) Transverse sections.

Figure 29.- Pressure distribution for the 20-inch nacelles in low position.

33

(a) Longitudinal sections.   (b) Transverse sections.

Figure 30.- Pressure distribution for the 34.7-inch nacelles.

REEL - C
358
A.T.I.
9322

Wilson, H. A.
Lehr, Robert, R.

AUTHOR(S)

DIVISION: Aerodynamics (2)
SECTION: Parasitic Components and Interference (7)
CROSS REFERENCES: Nacelles, Engine - Aerodynamics (66075);
Drag, Aerodynamic (31080); Nacelles,
Engine - Wind tunnel tests (66080)

AMER. TITLE: Drag and propulsive characteristics of air-cooled engine-nacelle installations
for two-engine airplanes

FORG'N. TITLE:

ORIGINATING AGENCY: National Advisory Committee for Aeronautics, Washington, D. C.

TRANSLATION:

COUNTRY	LANGUAGE	FORG'N.CLASS	U. S.CLASS.	DATE	PAGES	ILLUS.	FEATURES
U.S.	Eng.		Unclass.	Dec'40	33	30	photos, diagrs, graphs

ABSTRACT

Tests were made on model of a two-engined airplane provided with nacelles varying in
diameter from 1.5 to 2.6 times that of the local wing thickness. Results show variation
of nacelle drag with ratio of nacelle diameter to wing thickness, effects of nacelles on
aerodynamic characteristics of airplane, and propulsive and over-all efficiencies for all
arrangements. Present results are combined in some cases with results of previous experi-
ments so that effect of nacelles is included for airplanes ranging from 6-1/2 to 100 tons.

NOTE: Requests for copies of this report must be addressed to: N.A.C.A.,
Washington, D. C.

RESTRICTED (19 KAR 47)

Wilson, H. A.
Lehr, Robert, R.

AUTHOR(S)

DIVISION: Aerodynamics (2)
SECTION: Parasitic Components and Interference (7)
CROSS REFERENCES: Nacelles, Engine - Aerodynamics (66075);
Drag, Aerodynamic (31080); Nacelles,
Engine - Wind tunnel tests (66080)

ATI- 9322

ORIG. AGENCY NUMBER

ACR-L-428

REVISION

AMER. TITLE: Drag and propulsive characteristics of air-cooled engine-nacelle installation
for two-engine airplanes

FORG'N. TITLE:

ORIGINATING AGENCY: National Advisory Committee for Aeronautics, Washington, D. C.
TRANSLATION:

240 400

COUNTRY	LANGUAGE	FORG'N.CLASS	U. S.CLASS.	DATE	PAGES	ILLUS.	FEATURES
U.S.	Eng.		Unclass.	Dec'40	33	30	photos, diagrs, graphs

ABSTRACT

Tests were made on model of a two-engined airplane provided with nacelles varying in
diameter from 1.5 to 2.6 times that of the local wing thickness. Results show variation
of nacelle drag with ratio of nacelle diameter to wing thickness, effects of nacelles on
aerodynamic characteristics of airplane, and propulsive and over-all efficiencies for all
arrangements. Present results are combined in some cases with results of previous experi-
ments so that effect of nacelles is included for airplanes ranging from 6-1/2 to 100 tons.

NOTE: Requests for copies of this report must be addressed to: N.A.C.A.,
Washington, D. C.

AD-B804 797

INDEX

WRIGHT FIELD, OHIO, USAAF *M. W.*

P/11

Engine Nacelles
& Aerodynamic Drag